Carbohydrate Polymers 83 (2011) 1715–1722

Contents lists available at ScienceDirect

Carbohydrate Polymers

journal homepage: www.elsevier.com/locate/carbpol

Synthesis and anti-hepatitis B virus activity of acyclovir conjugated stearic acid-*g*-chitosan oligosaccharide micelle

Su-Ting Huang[a,b], Yong-Zhong Du[b], Hong Yuan[b], Xing-Guo Zhang[c], Jing Miao[c], Fu-De Cui[a,*], Fu-Qiang Hu[b,*]

[a] College of Pharmaceutical Sciences, Shenyang Pharmaceutical University, Shenyang 110016, PR China
[b] College of Pharmaceutical Sciences, Zhejiang University, Hangzhou 310058, PR China
[c] Department of Pharmacology, First Affiliated Hospital, Zhejiang University School of Medicine, Hangzhou 310003, PR China

ARTICLE INFO

Article history:
Received 9 September 2010
Received in revised form 13 October 2010
Accepted 14 October 2010
Available online 20 October 2010

Keywords:
Acyclovir
Chitosan oligosaccharide
Stearic acid
Polymeric micelle
Anti-hepatitis B virus

ABSTRACT

The controlled release of chemotherapeutical reagent with high water solubility was a challenge for targeting drug delivery. In this article, an antiviral agent, acyclovir was conjugated to chitosan-*g*-stearate via a succinate linker. Chitosan-*g*-stearate was synthesized by the reaction between the amino group of chitosan oligosaccharide and the carboxyl group of stearic acid. Both chitosan-*g*-stearate and acyclovir-chitosan-*g*-stearate could self aggregate to form micelles in aqueous solution. Acyclovir-chitosan-*g*-stearate micelle had smaller size (24.9 ± 1.1 nm), lower positive zeta potential (24.4 mV) and higher critical micelle concentration (123.23 mg mL^{-1}) in distilled water, compared with those of chitosan-*g*-stearate (34.2 ± 3.8 nm, 46.9 ± 6.2 mV and 90.07 mg mL^{-1}, respectively). Acyclovir release from acyclovir-chitosan-*g*-stearate micelles could prolong to 24 h *in vitro*. For the free acyclovir and acyclovir-chitosan-*g*-stearate micelle with acyclovir concentration of 0.044 μM mL^{-1}, the inhibition of acyclovir on hepatitis B surface antigen was increased from 12.7% to 22.3% from 5 d to 9 d, while the inhibition of acyclovir-chitosan-*g*-stearate was increased from 58.2% to 80.3% from 5 d to 9 d. The cellular uptake and antiviral activity of acyclovir was successfully increased and improved through chemical conjugation of acyclovir to chitosan-*g*-stearate.

1. Introduction

Antiviral agent had low drug specificity towards the affected organs, thus high doses are frequently needed for clinic. Excessive or insufficient water-solubility and low cellular internalization also reduce their bioavailability (Park, Saravanakumar, Kim, & Kwon, 2010). To overcome these problems, two main approaches have been used: the employment of new therapeutic substances with higher bioavailability or more efficient drug delivery systems (Torchilin, 2001).

Acyclovir, a synthetic purine nucleoside analogue, is the prototype antiviral agent, which is activated by viral thymidine kinase. Acyclovir triphosphate inhibits DNA synthesis by acting as a chain terminator and the inhibition activity of acyclovir is highly selective due to its special affinity for the thymidine kinase enzyme encoded by herpes simplex virus and varicella zoster virus (Suzuki, Okuda, & Shiraki, 2006), and its anti-hepatitis B virus activity has been reported (Feng, Cai, Huang, & Zhou, 2008). However, the average oral bioavailability of acyclovir is fairly low (only 10–20%) and its plasma elimination half-life is 2.5–3.3 h (Tao et al., 2009), which means that frequent administrations are needed to maintain therapeutic drug concentration. The low oral bioavailability of acyclovir can be explained mainly by its low diffusivity, because plasma membrane is the primary barrier to entering the cytosolic space (Saito, Swanson, & Lee, 2003).

The drug delivery system could change the *in vivo* distribution of drug. The distribution and elimination patterns depended mainly on its physicochemical properties, such as size, charge, hydrophilic/lipophilic balance, shape, flexibility and deformability and the anatomical characteristics of endothelial capillaries (Taylor & Granger, 1983).

Ideal drug carriers should be easily synthesized with low cost, freely water-soluble, non-toxic, non-immunogenic and well characterized from the physicochemical point of view (Matthews, Pouton, & Threadgill, 1996; Nagarwal, Shri, Singh, Maiti, & Pandit, 2009). Chitosan is a natural polysaccharide derived from chitin by alkaline deacetylation, which is regarded as non-toxic, low immunogenicity and biodegradable. Chitosan with low molecular weight was obtained by enzymatic degradation from chitosan, which indicated good water solubility in physiological pH condition (Ye et al., 2008). The chitosan-*g*-stearate was synthesized via coupling reaction between the amino groups of chitosan with low

* Corresponding authors. Tel.: +86 571 88208439; fax: +86 571 88208439.
E-mail addresses: cuifude@163.com (F.-D. Cui), hufq@zju.edu.cn (F.-Q. Hu).

0144-8617/$ – see front matter © 2010 Elsevier Ltd. All rights reserved.
doi:10.1016/j.carbpol.2010.10.032

molecular weight and carboxyl group of stearic acid (Hu, Ren, Yuan, Du, & Zeng, 2006). The chitosan-*g*-stearate could form micelles spontaneously in the aqueous medium, and could be rapidly internalized into cells (You, Hu, Du, Yuan, & Ye, 2007). Chitosan-*g*-stearate micelle had a hydrophobic core and hydrophilic shell, and it has been used as a potential carrier for antitumor drug in order to improve its antitumor activity (Hu et al., 2006; Hu, Wu, Du, You, & Yuan, 2008; You et al., 2007, 2008). However, it was proved that chitosan-*g*-stearate micelle was not suitable for physical entrapment of hydrophilic antiviral agent, such as acyclovir.

In this research, acyclovir was used as a model hydrophilic antiviral drug to conjugate with Chitosan-*g*-stearate micelle via succinic spacer (Colla, De Clercq, Busson, & Vanderhaeghe, 1983). The toxicity and antiviral activity of acyclovir and acyclovir-chitosan-g-stearate were carefully examined on $HepG_2$ cells and hepatitis B virus-transfected human hepatoma cells, respectively.

2. Materials and methods

2.1. Materials

Chitosan with about 5.0 kDa average weight average molecular weight was obtained by enzymatic degradation from 95% deacetylated chitosan (Mw 450.0 kDa), which was supplied by Yuhuan Marine Biochemistry Co., Ltd., China. Stearic acid was purchased from Shanghai Chemical Reagent Co., Ltd., China. 1-Ethyl-3-(3-dimethylaminopropyl) carbodiimide (EDC) and *N*-hydroxysuccinimide (NHS) were purchased from Shanghai Medpep Co., Ltd., China. 2,4,6-trinitrobenzene sulfonic acid and 3-(4,5-dimethylthiazol-2-yl)-2,5-diphenyltetrazolium bromide were purchased from Sigma Chemical Co., St. Louis, USA. Trypsin and DMEM medium were purchased from Gibco BRL, USA. Fetal bovine serum was purchased from Sijiqing Biologic, China. Acyclovir (9-[(2-hydroxyethoxy) methyl] guanine) was purchased from Xinxiang Pharmaceutical Co., Ltd., China; succinic anhydride was purchased from Jiangsu Yonghua Fine Chemicals Co., Ltd., China, *N*,*N*-dimethylformamide (DMF) was dried using CaH_2 and distilled under reduced pressure before use. Fluorescein isothiocyanate was purchased from Sigma (St. Louis, MO, USA). All other chemicals were analytical or chromatographic grade.

2.2. Synthesis of acyclovir-chitosan-g-stearate

2.2.1. Synthesis of chitosan-g-stearate

Chitosan-*g*-stearate was synthesized via the reaction between the carboxyl group of stearic acid with the amino groups of chitosan in the presence of EDC (Ye et al., 2008). Briefly, 0.25 g chitosan oligosaccharide was dissolved in 40 mL deionized water and 0.825 g stearic acid in 20 mL hot ethanol, respectively. They were then mixed at 80 °C under stirring. After 5.5 g EDC was added into the mixture, the coupling reaction was carried out for 5 h at 80 °C under stirring at 250 rpm. The final reaction solution was dialyzed against 10% ethanol solution using a dialysis membrane (molecular weight cutoff: 3.5 kDa, Spectrum Laboratories, Laguna Hills, CA) for 48 h with frequent exchange of fresh 10% ethanol solution to remove by-products. Finally, the dialyzed product was lyophilized (LABCONCO, FreeZone 2.5 Plus, USA).

2.2.2. Synthesis of O-succilylacyclovir

A mixture of 1.125 g (5 mmol) of acyclovir and 1.0 g (10 mmol) of succinic anhydride were dissolved in 75 mL dried DMF, and was then heated up to 60 °C in oil bath. After 0.71 mL triethylamine was added dropwise into the DMF solution, and the mixture was stirred for 21 h at 60 °C. After the solution was cooled to room temperature, the reaction mixture was evaporated under vacuum, and the residue was redissolved in 40 mL ice-water and acidified to pH 2.0 with 2 N HCl. The white precipitate was collected by filtration, washed thoroughly with ice-water, and dried in vacuo over P_2O_5 at 40 °C. The *O*-succilylacyclovir was then obtained by recrystallization from methanol.

2.2.3. Synthesis of acyclovir-chitosan-g-stearate

The acyclovir-chitosan-*g*-stearate was synthesized according the method reported by Jin, Qiao, Li, Ai, and Hou (2005). 40 mg of chitosan-*g*-stearate, 120 mg of EDC (0.62 mmol) and 70 mg of NHS (0.61 mmol) were dissolved in 80 mL distilled water and the pH value of the solution was adjusted to 6.5 by 0.2 M NaOH solution. Then 20 mg (0.061 mmol) of *O*-succilylacyclovir in 10 mL DMF was added dropwise to the mixture and stirred at room temperature for 24 h. The resulting product was purified by dialysis (molecular weight cutoff: 3.5 kDa, Spectrum Laboratories, Laguna Hills, CA) against PBS 7.4 (pH 7.4, 0.2 M $Na_2HPO_4{\cdot}2H_2O$, NaH_2PO_4, NaCl, KCl buffer solution) for 4 h and distilled water for 20 h to remove unreacted *O*-succilylacyclovir and other small molecules, and the solution was lyophilized to obtain the acyclovir-chitosan-*g*-stearate.

2.3. Chemical stability studies of O-succilylacyclovir

The hydrolysis of *O*-succilylacyclovir derivative was studied in buffer solutions at pH 1.2 (0.2 M HC1, NaC1), pH 5.6 (0.2 M CH_3COOH, CH_3COONa) and PBS 7.4 at 37 ± 0.1 °C. The rate of hydrolysis at different pH was monitored by determining the amount of acyclovir and *O*-succilylacyclovir with HPLC method. Each experiment was repeated in triplicate.

2.4. Characterization of chitosan-g-stearate and acyclovir-chitosan-g-stearate

2.4.1. ^1H NMR analysis

The ^1H NMR spectra of chemicals were obtained by an NMR spectrometer (AC-80, Bruker Biospin, Germany). Acyclovir and *O*-succilylacyclovir were dissolved in DMSO-d_6; chitosan-*g*-stearate and acyclovir-chitosan-*g*-stearate were dissolved in D_2O.

2.4.2. Determination of substitution degree for chitosan-g-stearate

Substitution degree (SD%) of chitosan-*g*-stearate, defined as the number of stearic acid groups per 100 anhydroglucose units of chitosan, was determined by the 2,4,6-trinitrobenzene sulfonic acid method (Andres & Martina, 1998). Four milligram chitosan-*g*-stearate were suspended in 1 mL distilled water and incubated with 2 mL 4% (w/v) $NaHCO_3$ and 2 mL 0.1% (w/v) 2,4,6-trinitrobenzene sulfonic acid under 37 ± 0.1 °C for 2 h. Then, 2 mL 2 N HCl was added. The ultra-violet (UV) absorbance of sample at 344 nm was measured by a UV spectroscopy (TU-1800PC, Beijing Purkinje General Instrument Co., Ltd., China). The substitution degree of chitosan-*g*-stearate was calculated using a calibration curve obtained by the amino-group determination of a series of solutions with different concentrations.

2.4.3. Size and zeta potential

The hydrodynamic diameters and zeta potential of chitosan-*g*-stearate and acyclovir-chitosan-*g*-stearate micelle solution (1 mg mL^{-1}) were measured by the Zetasizer (3000 HS, Malvern Instruments Ltd., UK).

2.4.4. Transmission electron microscopy investigation

The morphological examinations of the chitosan-*g*-stearate and acyclovir-chitosan-*g*-stearate micelles were performed by a transmission electron microscopy (TEM) (JEOL JEM-1230, Japan). The

samples were stained with 2% (w/v) phosphotungstic acid and placed on copper grids with films for viewing by TEM.

2.4.5. Critical micelle concentration of chitosan-g-stearate and acyclovir-chitosan-g-stearate

The critical micelle concentration of the synthesized chitosan-*g*-stearate and acyclovir-chitosan-*g*-stearate in pH 7.4 PBS was estimated by a fluorescence spectroscopy using pyrene as a probe (Slaughter, Schmidt, Byram, & Mecozzi, 2007). Fluorometer (F-2500, Hitachi Co., Japan) was used to record fluorescence spectra, and the excitation wavelength 337 nm, the slit were set at 2.5 nm (excitation) and 10 nm (emission). The intensities of the emission were monitored at a wavelength range of 360–450 nm. The concentration of chitosan-*g*-stearate and acyclovir-chitosan-*g*-stearate solution containing 5.93×10^{-7} M of pyrene was varied from 1.0 to 1×10^{3} μg mL^{-1}. Then the ratio of the intensities (I_1/I_3) of the first peak (I_1, 374 nm) to the third peak (I_3, 385 nm) was calculated.

2.4.6. Determination of the acyclovir content in acyclovir-chitosan-g-stearate

The acyclovir content in acyclovir-chitosan-*g*-stearate was proved by the ^{1}H NMR spectroscopy and confirmed by alkaline hydrolysis with HPLC analysis. Equal volume of 0.2 M NaOH solution was added in acyclovir-chitosan-*g*-stearate micelle solution (1 mg mL^{-1}), which was maintained at 37 ± 0.1 °C and shaken horizontally at 66 rpm for 2 h. Subsequently, the supernatant was obtained using centrifugation at 35,000 rpm for 10 min. The concentration of acyclovir in the supernatant, which was alkaline hydrolyzed from the conjugate was determined by HPLC analysis (column, Hypersil ODS, 5 μm of 150 mm × 4.6 mm i.d., purchased from Dalian Elite Analytical Instruments Co., Ltd., China; flow rate, 1 mL min^{-1}; injection volume, 20 μL; mobile phase, CH_3OH: CH_3COONa 20 mM (pH 5.6 with CH_3COOH) 10:90; detection wavelength, 254 nm) (Giammona, Puglisi, Cavallaro, Spadaro, & Pitarresi, 1995).

2.5. In vitro drug release study from acyclovir-chitosan-g-stearate

in vitro drug release experiments were carried out as follows: 1.0 mL acyclovir-chitosan-*g*-stearate solution (1.0 or 0.1 mg mL^{-1}) was added into a dialysis membrane (molecular weight cutoff: 3.5 kDa, Spectrum Laboratories, Laguna Hills, CA), and then placed in a plastic tube containing 10 mL pH 7.4 PBS solution. The tests were conducted in incubator shaker (HZ-88125, Scientific and Educational Equipment Plant, Taicang, China), which was maintained at 37 ± 0.1 °C and shaken horizontally at 66 rpm. At predetermined time, the media was removed and replaced with fresh PBS solution. The amount of released drug was determined by HPLC. For comparison, free acyclovir released from a dialysis membrane was conducted in the same condition. Each experiment was repeated in triplicate.

2.6. Cellular uptake of fluorescent chitosan-g-stearate and acyclovir-chitosan-g-stearate

$HepG_2$ cell line (kindly provided by the State Key Lab for Diagnosis and Treatment of Infectious Diseases, Zhejiang University, China) was used as model cells to evaluate the cellular uptake ability. This cells were cultured at 37 ± 0.1 °C in DMEM supplemented with 10% (w/w) fetal bovine serum and 500 μg mL^{-1} G418 in a humidified atmosphere containing 5% (v/v) CO_2.

At first, the chitosan-*g*-stearate and acyclovir-chitosan-*g*-stearate micelles were labeled with fluorescein isothiocyanate via the reaction of amino groups of chitosan and isothiocyanate groups of fluorescein isothiocyanate. The modification ratio of fluorescein isothiocyanate to chitosan-*g*-stearate or acyclovir-chitosan-*g*-stearate was 1:1. $HepG_2$ cells were seeded in a 24-well plate at a seeding density of 10,000 cells per well with 1 mL of growth medium each well and incubated for 24 h to attach them completely. Cells were further incubated with culture medium containing fluorescein isothiocyanate labeled chitosan-*g*-stearate and acyclovir-chitosan-*g*-stearate (the concentration was 100 μg mL^{-1}) at 37 ± 0.1 °C. After different incubation time, the culture medium was removed and the cells were washed twice with pH 7.4 PBS solution and directly viewed under a fluorescence microscope (OLYMPUS America, Melville, NY, USA).

2.7. In vitro anti-hepatitis B virus activity

$HepG_2$ 2.2.15 cells, hepatitis B virus-transfected human hepatoma cells, were used to perform anti-hepatitis B virus activity *in vitro* (Kayhan et al., 2006). The cell line was kindly provided by the State Key Lab for Diagnosis and Treatment of Infectious Diseases, Zhejiang University, China. The cells were cultured at 37 ± 0.1 °C in DMEM supplemented with 10% (w/w) fetal bovine serum and 500 μg mL^{-1} G418 in a humidified atmosphere containing 5% (v/v) CO_2.

Cells were seeded in 24-well plates. After incubation for 48 h, drug dissolved in distilled water was added into culture medium with the given concentration and cultured continually for 5 and 9 d. After incubation, the culture media in the wells was collected for the virological assessment, and the survival of cells were determined by MTT method. Briefly, at the end of incubation time, 60 μL of MTT solution with the concentration of 5 mg mL^{-1} was added and incubated for further 4 h at 37 ± 0.1 °C. Each well was then washed with 50 μL PBS after the medium containing un-reacted MTT was removed, and then 100 μL DMSO was added to each well to dissolve the MTT formazan crystals. Finally, the plates were shaken for 20 min, transferred to 96-well plates and the absorbance of formazan product was measured at 570 nm in a microplate reader (Bio-Rad, Model 680, USA). Hepatitis B surface antigen and hepatitis B e antigen productions in culture media were determined by commercial enzyme immunoassay kits (AXSYM System, Abbott, Wiesbaden, Germany). Hepatitis B virus DNA was quantified by a commercial real-time polymerase chain reaction (PCR) kit (PG Biotech., Shenzhen, China). The OD (optical density) was determined with hepatitis B surface antigen and hepatitis B e antigen kit and calculated as:

$$\text{The inhibition rate} = \frac{\text{OD(control cells)} - \text{OD(test cells)}}{\text{OD(control cells)}}.$$

All the experiments were performed in triplicate.

2.8. Statistical analysis

Data were expressed as mean of three separate experiments, and was compared by analysis of variance (ANOVA). $P < 0.05$ was considered statistically significant in all cases.

3. Results and discussion

3.1. Synthesis of acyclovir-chitosan-g-stearate

The synthesis route was shown in Fig. 1A. *O*-succilylacyclovir was obtained with about 56% yield after recrystallization from methanol. The ^{1}H NMR spectra were shown in Fig. 1B–E, and were in agreement with the previous report (Colla et al., 1983). In ^{1}H NMR spectrum of acyclovir (Fig. 1B), the peak at 7.9 ppm was attributed to the proton of pyridine in acyclovir (N=C**H**–N); in ^{1}H NMR spectrum of *O*-succilylacyclovir (Fig. 1C), the peaks at 12.2 ppm was

attributed to the proton of (CH_2–COO**H**) in the succinic anhydride linkage. The characteristics of the purified *O*-succilylacyclovir demonstrated that the adopted chemical procedure for the succinyl intermediate synthesis was efficient for the high purity degree.

The chemical stability of the *O*-succilylacyclovir was studied under different pH condition using buffer solution with pH 1.2, pH 5.6 and pH 7.4 at 37 ± 0.1 °C. The results were indicated in Fig. 2. In the buffer solution, the *O*-succilylacyclovir was hydrolyzed to acyclovir. It was found that the hydrolysis rate of *O*-succilylacyclovir was slowest in the pH 5.6 buffer solution, and increased in the order of pH values 5.6 < 7.4 < 1.2. The results might be due to the pKa of acyclovir. The pKa values of hydroxyl group and amino group of acyclovir were 2.27 and 9.25, respectively. It was reported that acyclovir was more stable in pH 5.6 than in other pH (Giammona et al., 1995).

The SD% of resulted chitosan-*g*-stearate measured by 2,4,6-trinitrobenzene sulfonic acid method was about 10.43 ± 0.29%, which was confirmed by ^{1}H NMR spectrum (Fig. 1D).

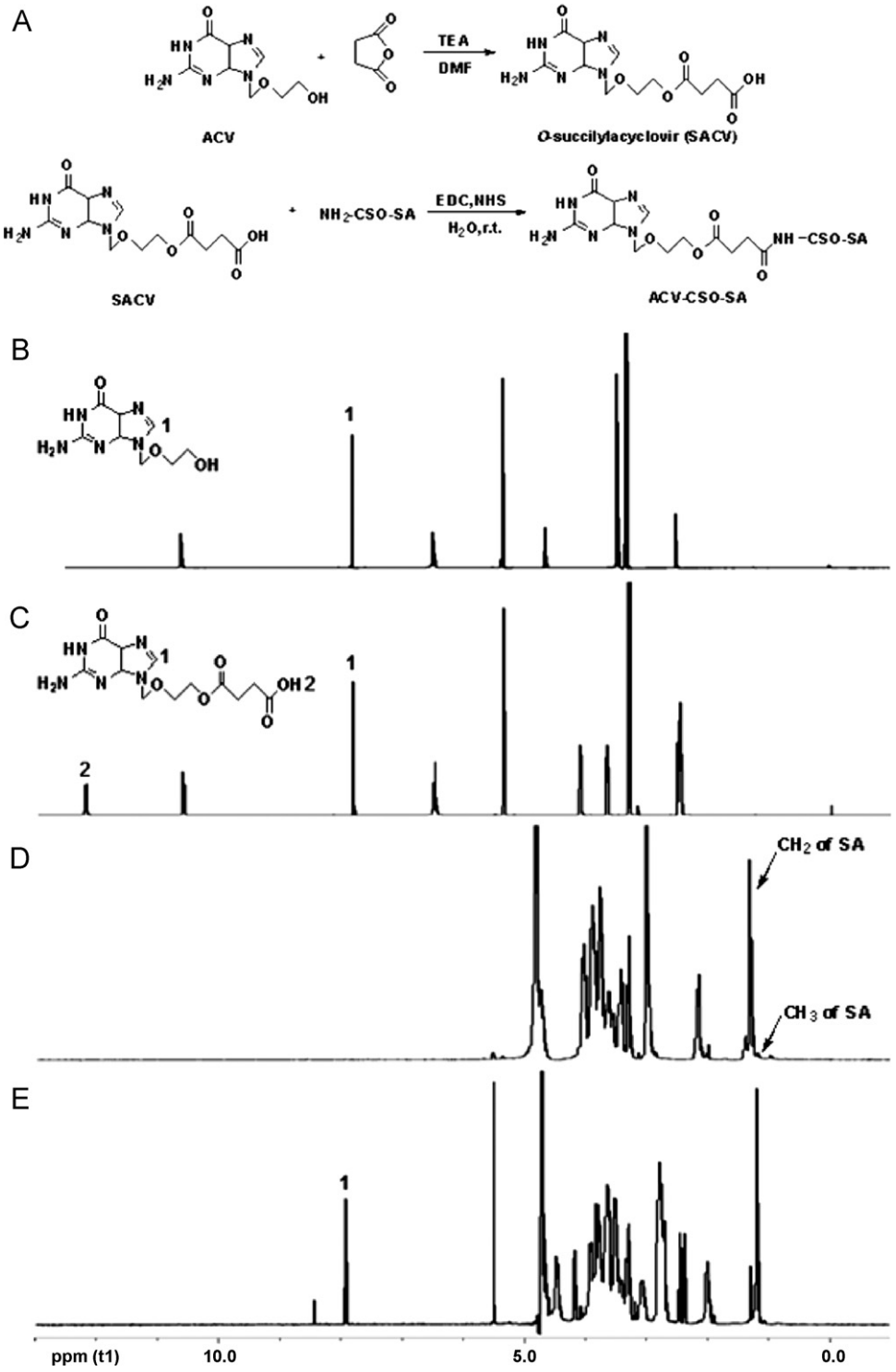

Fig. 1. (A) Synthesis routes of *O*-succilylacyclovir (SACV) and acyclovir-chitosan-*g*-stearate (ACV-CSO-SA). ^{1}H NMR spectra of acyclovir (B), *O*-succilylacyclovir (C), chitosan-*g*-stearate (CSO-SA) (D), and acyclovir-chitosan-*g*-stearate (E). SA in (D) and (E) presents stearic acid.

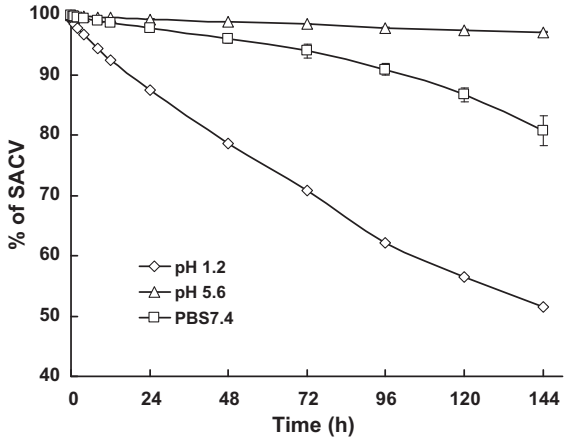

Fig. 2. Chemical stability of *O*-succilylacyclovir (SACV) in buffer solutions PBS pH 7.4 (□), pH 5.6 (△) and pH 1.2 (◊). Data represent the mean ± standard deviation ($n = 3$).

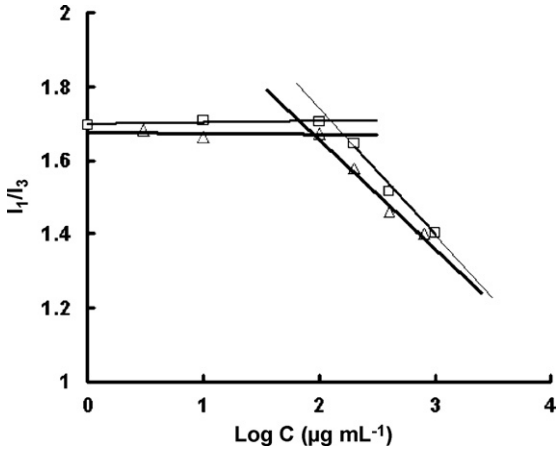

Fig. 3. Variation of intensity ratio (I_1/I_3) against logarithm of chitosan-*g*-stearate (CSO-SA) (△) and acyclovir-chitosan-*g*-stearate (ACV-CSO-SA) (□) concentration.

The synthesis route was shown in Fig. 1A, D and E show that the ^{1}H NMR spectra of chitosan-*g*-stearate and acyclovir-chitosan-*g*-stearate were almost the same, excepting the proton peak of pyridine of acyclovir (N═C**H**–N) in Fig. 2E. The structure of acyclovir-chitosan-*g*-stearate was verified by the ^{1}H NMR spectroscopy and the content of acyclovir was confirmed by alkaline hydrolysis with HPLC analysis, which was calculated to be about 9.0% (w/w).

The pKa of chitosan-*g*-stearate was approximately 6.5, which meant that there would be more active amino groups available for reaction in alkaline environment (Du, Lu, Zhou, Yuan, & Hu, 2010). However, the catalytic efficiency of EDC present pH dependence, and the relationship between catalytic efficiency and pH value exhibit "bell" shaped with pK's equal to 4.5 and 3.1 (Williams & Ibrahim, 1981). Therefore, considering catalytic efficiency of EDC, stability of *O*-succilylacyclovir in different pH buffer solutions and protonation of amino groups of chitosan oligosaccharide, the pH value of reacting solution was adjusted to 6.5 by addition of 0.2 M NaOH solution and 10 times molar of EDC. Considering low yields in the case of using EDC as a coupling agent, the coupling reactivity was improved with combination of NHS to enhance the stability of intermediate by avoiding hydrolysis in water (Staros, Wright, & Swingle, 1986).

3.2. Characteristics of chitosan-g-stearate and acyclovir-chitosan-g-stearate

The physicochemical properties of obtained chitosan-*g*-stearate and acyclovir-chitosan-*g*-stearate are shown in Table 1 and Fig. 3. It was clear that compared with chitosan-*g*-stearate, the critical micelle concentration, micellar size, polydispersity index of the micelle size and zeta potential of acyclovir-chitosan-*g*-stearate only changed slightly.

The spontaneous aggregation ability indicated by critical micelle concentration is an important characteristic for amphiphilic copolymer. The critical micelle concentration of chitosan-*g*-stearate and acyclovir-chitosan-*g*-stearate was investigated by a fluorescence spectroscopy with pyrene as a probe. Fig. 3 shows the variation I_1/I_3 against the logarithm of chitosan-*g*-stearate or acyclovir-chitosan-*g*-stearate concentration. At the lower concentration, the value of I_1/I_3 kept constant. It decreased when pyrene molecules were preferably partitioned into the less polar hydrophobic core due to the formation of micelles. From Table 1, it was obvious that the critical micelle concentration value slightly increased after the acyclovir was conjugated with chitosan-*g*-stearate.

As shown in Table 1, it was also found that the acyclovir-chitosan-*g*-stearate micelle had smaller size (24.9 ± 1.1 nm) and higher positive zeta potential in distilled water. After the acyclovir was conjugated with chitosan-*g*-stearate, the number average micellar size slightly decreased, while the zeta potential slightly increased due to the conjugation of acyclovir. Fig. 4 indicates the size distribution obtained by DLS determination and TEM images of the chitosan-*g*-stearate and acyclovir-chitosan-*g*-stearate micelles. The size of chitosan-*g*-stearate micelle was below 50 nm, while the size of acyclovir-chitosan-*g*-stearate micelle was near 20 nm. However, the micelle size obtained by DLS determination seemed larger than those observed from TEM images, which might be due to the shrink of hydrophilic backbone in the micelle during the dry process of TEM sample (Chen, Fan, Huang, Liu, & Sun, 2009).

3.3. In vitro drug release study

The drug release of acyclovir-chitosan-*g*-stearate was investigated by monitoring the presence of free acyclovir in the dissolution medium. The *in vitro* acyclovir release behaviors of acyclovir-chitosan-*g*-stearate with different concentrations were shown in Fig. 5. As shown in Fig. 5, approximate 68% of acyclovir was released from the polymeric conjugate with 0.1 mg mL^{-1} concentration after 24 h, while nearly 100% of the free drug was released within 4 h. Moreover, the drug release rate from acyclovir-chitosan-*g*-stearate increased with the decreasing acyclovir-chitosan-*g*-stearate concentration in dissolution medium. This might be due to the relative loose structure of acyclovir-chitosan-*g*-stearate micelle at lower concentration. In the case of acyclovir, a water-soluble drug, chemical conjugating to polymeric micelle such as chitosan-*g*-stearate micelle offered the possibility of prolonging the drug's half-time

Table 1
Characteristics of synthesized chitosan-*g*-stearate and acyclovir-chitosan-*g*-stearate micelle.

Micelle	Size by number (nm)	PI	Zeta (mV)	Critical micelle concentration (μg mL^{-1})
Chitosan-*g*-stearate	34.2 ± 3.8	0.607 ± 0.106	46.9 ± 6.2	90.07
Acyclovir-chitosan-*g*-stearate	24.9 ± 1.1	0.575 ± 0.019	24.4 ± 5.3	123.23

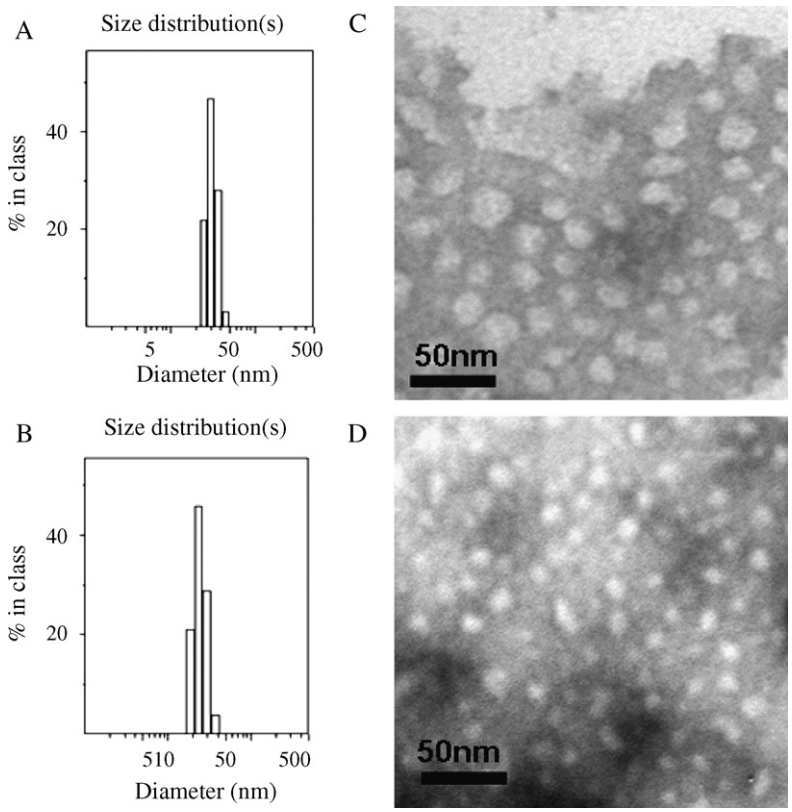

Fig. 4. Size distributions and TEM images of chitosan-*g*-stearate and acyclovir-chitosan-*g*-stearate micelles. Size distribution of chitosan-*g*-stearate (A); size distribution of acyclovir-chitosan-*g*-stearate (B); TEM image of chitosan-*g*-stearate (C); and TEM image of acyclovir-chitosan-*g*-stearate (D).

and increasing its bioavailability, and facilitated cellular uptake to improve the therapeutic efficacy.

3.4. Cellular uptake of chitosan-g-stearate and acyclovir-chitosan-g-stearate

Fig. 6 shows the fluorescence images of the $HepG_2$ cells after the cells were incubated with fluorescein isothiocyanate labeled chitosan-*g*-stearate and acyclovir-chitosan-*g*-stearate for 24 h at the same incubation concentration of 100 $\mu g\,mL^{-1}$. As shown in Fig. 6, after the chitosan-*g*-stearate was conjugated with acyclovir, the acyclovir-chitosan-*g*-stearate could also be uptaken by cells, and no significant difference was found between chitosan-*g*-stearate and acyclovir-chitosan-*g*-stearate.

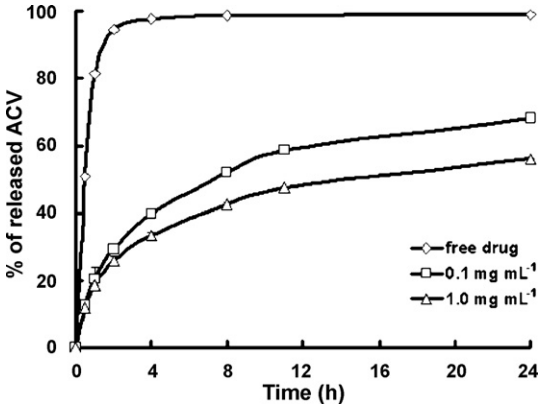

Fig. 5. *In vitro* acyclovir release behaviors from acyclovir-chitosan-*g*-stearate at different acyclovir-chitosan-*g*-stearate concentrations. Data represent the mean ± standard deviation ($n = 3$).

3.5. Anti-hepatitis B virus activity in vitro

At first, the cytotoxocities of chitosan-*g*-stearate and acyclovir-chitosan-*g*-stearate were evaluated by determining the 50% inhibition of cellular growth (IC_{50}) of chitosan-*g*-stearate and acyclovir-chitosan-*g*-stearate. The IC_{50} of chitosan-*g*-stearate and acyclovir-chitosan-*g*-stearate micelles against $HepG_2$ 2.2.15 cell line measured by MTT method was higher than 1000 $\mu g\,mL^{-1}$.

The hepatitis B virus inhibition rates determined by hepatitis B e antigen, hepatitis B surface antigen and hepatitis B virus DNA assays of acyclovir, *O*-succilylacyclovir and acyclovir-chitosan-*g*-stearate were shown in Fig. 7. From Fig. 7A, it was found that after 9 d, the inhibition activities of free acyclovir and *O*-succilylacyclovir solution on hepatitis B virus-induced hepatitis B surface antigen and hepatitis B e antigen increased nearly 1 time when the concentration increased from 0.044 to 0.44 $\mu M\,mL^{-1}$, the inhibition of acyclovir on hepatitis B e antigen was higher than that of *O*-succilylacyclovir. In contrast, the inhibition of acyclovir on hepatitis B surface antigen was lower than that of *O*-succilylacyclovir. Both acyclovir and *O*-succilylacyclovir with concentration of 0.44 $\mu M\,mL^{-1}$ showed high inhibitory activities on hepatitis B virus DNA. The results indicated that *O*-succilylacyclovir itself owned obvious antiviral activity on hepatitis B surface antigen, hepatitis B e antigen and hepatitis B virus DNA.

As shown in Fig. 7B, for the free acyclovir with concentration of 0.044 $\mu M\,mL^{-1}$, the inhibition on hepatitis B surface antigen was increased from 12.7% to 22.3% from 5 d to 9 d; for acyclovir-chitosan-*g*-stearate micelle loading 0.044 $\mu M\,mL^{-1}$ acyclovir, the inhibition was increased from 58.2% to 80.3% from 5 d to 9 d. It was clear that the inhibition activities of acyclovir-chitosan-*g*-stearate micelle were much higher than that of free acyclovir, which contained the same amount of acyclovir. Acyclovir-chitosan-*g*-stearate micelle had higher efficiency of inhibition activities on both hepati-

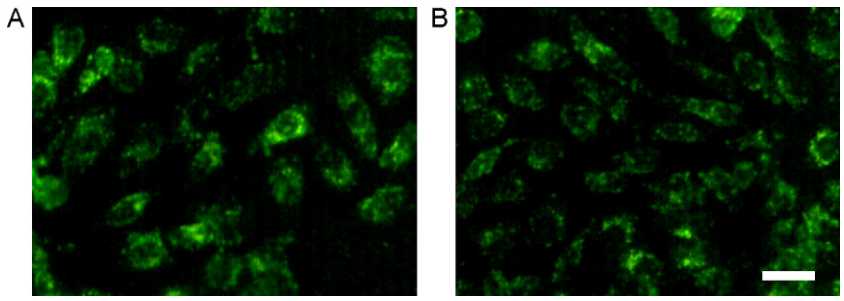

Fig. 6. Fluorescence images after the cells were incubated with the fluorescein isothiocyanate labeled chitosan-*g*-stearate (A) and acyclovir-chitosan-*g*-stearate (B) for 24 h. The bar is 10 μm.

tis B surface antigen and hepatitis B e antigen expressions than that of free acyclovir after incubated with $HepG_2$ 2.2.15 cells for both 5 d and 9 d ($P < 0.05$). It also indicated that the acyclovir-chitosan-g-stearate micelle could inhibit the production of hepatitis B virus DNA more significantly (nearly 100%) than free acyclovir (less than 30%) after incubated with $HepG_2$ 2.2.15 cells for both 5 d and 9 d ($P < 0.05$). It can be concluded that acyclovir-chitosan-*g*-stearate micelle showed higher anti-hepatitis B virus activity than the free drug due to the excellent cellular internalization ability.

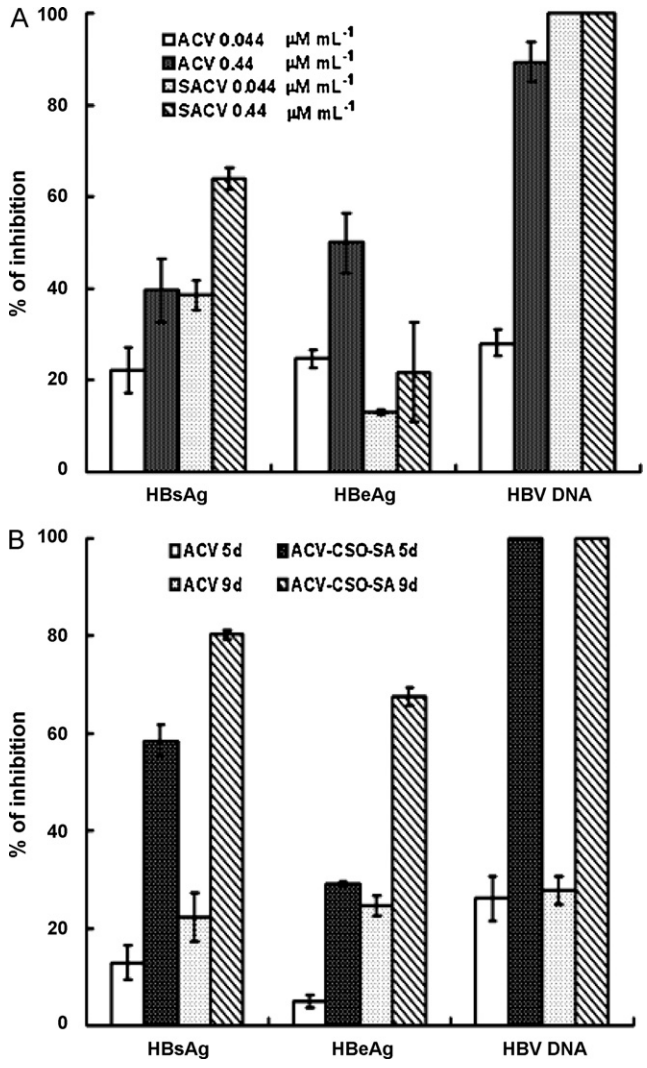

Fig. 7. *In vitro* activities of hepatitis B virus (HBV), hepatitis B surface antigen (HBsAg) and hepatitis B e antigen (HBeAg) on $HepG_2$ 2.2.15 cells. Data represent the mean ± standard deviation ($n = 3$). ACV, SACV, ACV-CSO-SA indicate acyclovir, *O*-succilylacyclovir and acyclovir-chitosan-*g*-stearate, respectively.

4. Conclusions

Antiviral agent such as acyclovir had low oral bioavailability, and high doses were usually administrated to reach the desired therapeutic effect. The structure modification of antiviral agent and the employing of effective drug delivery system are the main route to improve the drug bioavailability and reduce the drug dose. Here, acyclovir was successfully conjugated to chitosan-*g*-stearate micelles via a succinate linker. The acyclovir-chitosan-*g*-stearate micelles had nano-scaled size and kept the cellular internalization ability of chitosan-*g*-stearate. *in vitro* acyclovir release from acyclovir-chitosan-g-stearate could prolong to 24 h. The acyclovir-chitosan-*g*-stearate micelles indicated higher anti-hepatitis B virus activity including the expressions of hepatitis B surface antigen, hepatitis B e antigen and hepatitis B virus DNA than those of the free drug *in vitro*. These results would be helpful for designing chitosan-*g*-stearate as a nano-carrier of other hydrophilic antiviral agents and improving therapeutic efficacy of chronic hepatitis.

Acknowledgements

We are grateful for financial support of National Basic Research Program of China (973 Program) under contract 2009CB930300, National HighTech Research and Development Program (863) of China (2007AA03Z318), and Foundation of Science and Technology Department of Zhejiang Province (2008C23043).

References

Andres, B. S., & Martina, E. K. (1998). Mucoadhesive polymers as platforms for peroral peptide delivery and absorption: Synthesis and evaluation of different chitosan EDTA conjugates. *Journal of Controlled Release*, *50*, 215–223.

Chen, W. X., Fan, X. D., Huang, Y., Liu, Y. Y., & Sun, L. (2009). Synthesis and characterization of a pentaerythritol-based amphiphilic star block copolymer and its application in controlled drug release. *Reactive and Functional Polymers*, *69*, 97–104.

Colla, L., De Clercq, E., Busson, R., & Vanderhaeghe, H. (1983). Synthesis and antiviral activity of water-soluble esters of acyclovir [9-[(2-hydroxyethoxy)methyl]guanine]. *Journal of Medical Chemistry*, *26*, 602–604.

Du, Y. Z., Lu, P., Zhou, J. P., Yuan, H., & Hu, F. Q. (2010). Stearic acid grafted chitosan oligosaccharide micelle as a promising vector for gene delivery system: Factors affecting the complexation. *International Journal of Pharmaceutics*, *391*, 260–266.

Feng, M. Q., Cai, Q. S., Huang, H., & Zhou, P. (2008). Liver targeting and anti-HBV activity of reconstituted HDL–acyclovir palmitate complex. *European Journal of Pharmaceutics and Biopharmaceutics*, *68*, 688–693.

Giammona, G., Puglisi, G., Cavallaro, G., Spadaro, A., & Pitarresi, G. (1995). Chemical stability and bioavailability of acyclovir coupled to α,β-poly(*N*-2-hydroxyethyl)-DL-aspartamide. *Journal of Controlled Release*, *33*, 261–271.

Hu, F. Q., Ren, G. F., Yuan, H., Du, Y. Z., & Zeng, S. (2006). Shell cross-linked stearic acid grafted chitosan oligosaccharide self-aggregated micelles for controlled release of paclitaxel. *Colloids and Surfaces B-Biointerfaces*, *50*, 97–103.

Hu, F. Q., Wu, X. L., Du, Y. Z., You, J., & Yuan, H. (2008). Cellular uptake and cytotoxicity of shell crosslinked stearic acid grafted chitosan oligosaccharide micelles encapsulating doxorubicin. *European Journal of Pharmaceutics and Biopharmaceutics*, *69*, 117–125.

Jin, Y. G., Qiao, Y. X., Li, M., Ai, P., & Hou, X. P. (2005). Langmuir monolayers of the long-chain alkyl derivatives of a nucleoside analogue and the formation of self-assembled nanoparticles. *Colloids and Surfaces B-Biointerfaces*, *42*, 45–51.

Kayhan, H., Karatayli, E., Turkyilmaz, A. R., Sahin, F., Yurdaydin, C., & Bozdayil, A. M. (2006). Inhibition of hepatitis B virus replication by shRNA in stably HBV expressing HEPG2 2.2.15 cell lines. *Journal of Hepatology*, *44*, S147.

Matthews, S. E., Pouton, C. W., & Threadgill, M. D. (1996). Macro molecular systems for chemotherapy and magnetic imaging. *Advanced Drug Delivery Reviews*, *18*, 219–267.

Nagarwal, R. C., Shri, K., Singh, P. N., Maiti, P., & Pandit, J. K. (2009). Polymeric nanoparticulate system: A potential approach for ocular drug delivery. *Journal of Controlled Release*, *136*, 2–13.

Park, J. H., Saravanakumar, G., Kim, K., & Kwon, I. C. (2010). Targeted delivery of low molecular drugs using chitosan and its derivatives. *Advanced Drug Delivery Reviews*, *62*, 28–41.

Saito, G., Swanson, J. A., & Lee, K. D. (2003). Drug delivery strategy utilizing conjugation via reversible disulfide linkages: Role and site of cellular reducing activities. *Advanced Drug Delivery Reviews*, *55*, 199–215.

Slaughter, J. N., Schmidt, K. M., Byram, J. L., & Mecozzi, S. (2007). Synthesis and self-assembly properties of a novel [poly(ethylene glycol)]-fluorocarbon-phospholipids triblock copolymer. *Tetrahedron Letters*, *48*, 3879–3882.

Staros, J. V., Wright, R. W., & Swingle, D. M. (1986). Enhancement by *N*-hydroxysulfosuccinimide of water-soluble carbodiimide-mediated coupling reactions. *Analytical Biochemistry*, *156*, 220–222.

Suzuki, M., Okuda, T., & Shiraki, K. (2006). Synergistic antiviral activity of acyclovir and vidarabine against herpes simplex virus types 1 and 2 varicella-zoster virus. *Antiviral Research*, *72*, 157–161.

Tao, Y. Y., Lu, Y. F., Sun, Y. J., Gu, B., Lu, W. Y., & Pan, J. (2009). Development of mucoadhesive microspheres of acyclovir with enhanced bioavailability. *International Journal of Pharmaceutics*, *378*, 30–36.

Taylor, A. E., & Granger, D. N. (1983). Equivalent pore modeling vesicles and channels. *Federation Proceedings*, *42*, 2440–2445.

Torchilin, V. P. (2001). Structure and design of polymeric surfactant-based drug delivery systems. *Journal of Controlled Release*, *73*, 137–172.

Williams, A., & Ibrahim, T. (1981). A new mechanism involving cyclic tautomers for the reaction with nucleophiles of the water-soluble peptide coupling reagent EDC. *Journal of the American Chemistry Society*, *103*, 7090–7095.

Ye, Y. Q., Yang, F. L., Hu, F. Q., Du, Y. Z., Yuan, H., & Yu, H. Y. (2008). Core-modified chitosan based polymeric micelles for controlled release of doxorubicin. *International Journal of Pharmaceutics*, *352*, 294–301.

You, J., Hu, F. Q., Du, Y. Z., Yuan, H., & Ye, B. F. (2007). High cytotoxicity and resistant-cell reversal of novel paclitaxel loaded micelles by enhancing molecular-target delivery of the drug. *Nanotechnology*, *18*, 495101.

You, J., Li, X., Cui, F. D., Du, Y. Z., Yuan, H., & Hu, F. Q. (2008). Folate conjugated polymer micelles for active-targeting to cancer cells: Preparation, in vitro evaluation of targeting ability and cell cytotoxicity. *Nanotechnology*, *19*, 045102.